

Progress presentation

Algorithm development for the segmentation of astronomical
images with unique features

Viktor Nagy

Space Debris

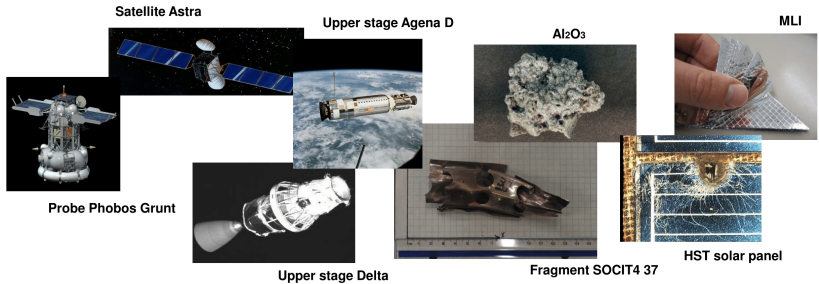


Figure 1: Space debris sources

Space View

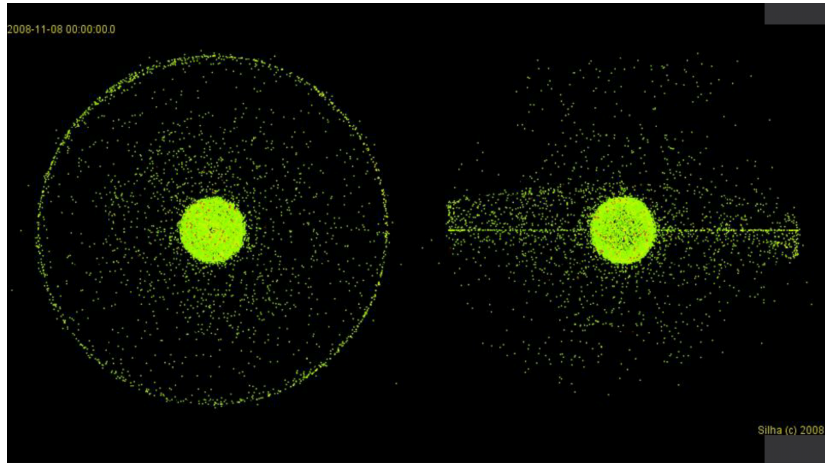


Figure 2: Debris clusters (GEO, LEO)

GEO/LEO

There are multiple orbital layers

- LEO (Low Earth Orbit)
- GEO (Geosynchronous Earth Orbit)
- GNSS, GTO, Molniya

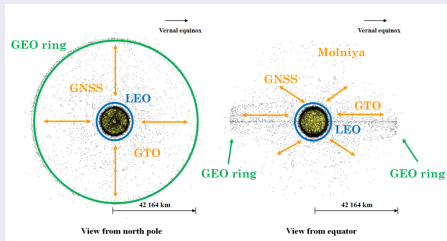


Figure 3: Orbital layers

Change over time

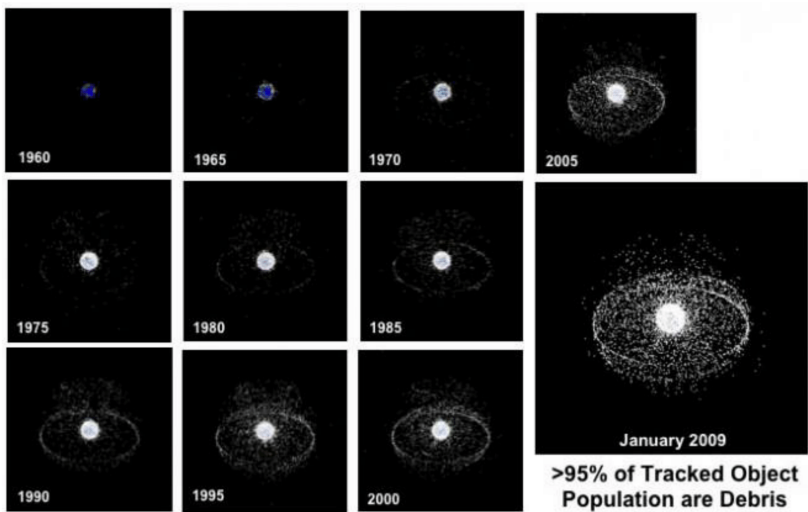


Figure 4: Amount of debris through time milestones

AGO 70cm

AGO 70 programs

- Astrometry, surveys
- Photometry, light curves
- Photometry, colors



Figure 5: AGO 70cm installation(left), mount(middle), primary mirror(right)

Pipeline

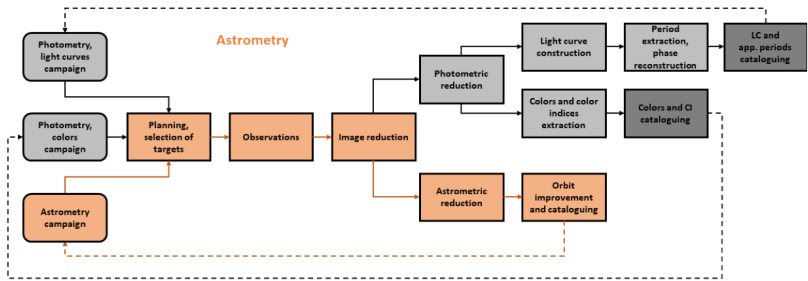


Figure 6: Astrometry pipeline

Tracking

There are 2 types of tracking

- Sidereal tracking
- Object tracking

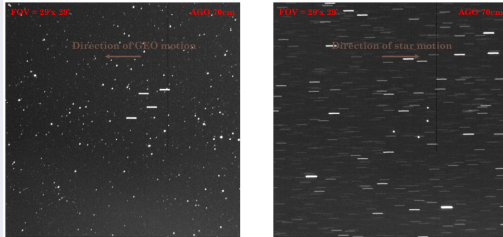


Figure 7: Possible tracking methods, Sidereal tracking(left), Object tracking(right)

Steps

- Image capture
- Image reduction
- Sky background estimation/extraction
- Objects search and centroiding
- Star field identification
- Astrometric reduction
- Star Masking
- Tracklet building
- Object identification
- Data format transformation
- Output data redistribution

Sky background estimation/subtraction

Reasons/Causes

- Moon light (global linear gradient)
- Stars, Nebulas, Galaxies (local nonlinear gradients)
- Hardware related reflexions

Methods

- Convolution with large median kernel (at least 25% of the size of image)
- Sigma clipping

Sky background estimation/subtraction

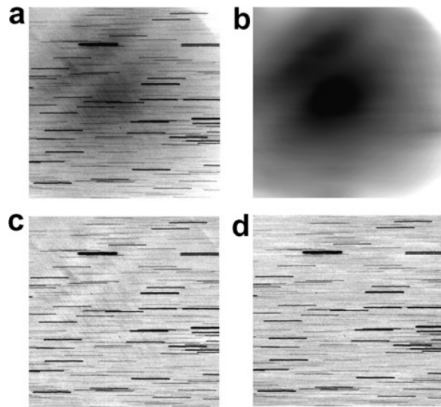


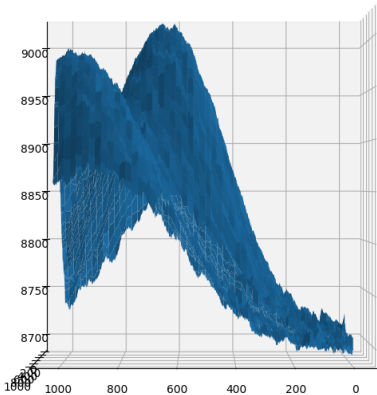
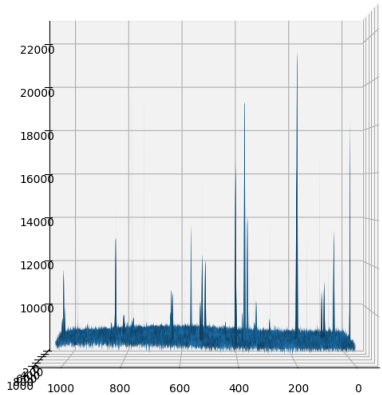
Figure 8: original image(a), background(b), result median filtering(c), sigma clipping(d)

Sky background estimation/subtraction



Figure 9: Dumbbell nebula M27, AGO 70cm telescope

Sky background estimation results



Object identification

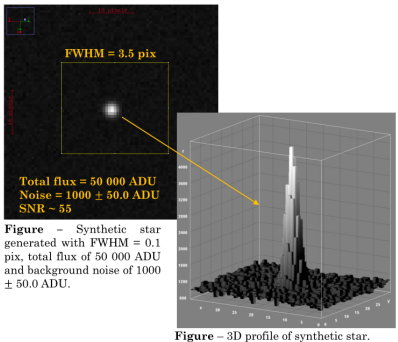


Figure – 3D profile of synthetic star.

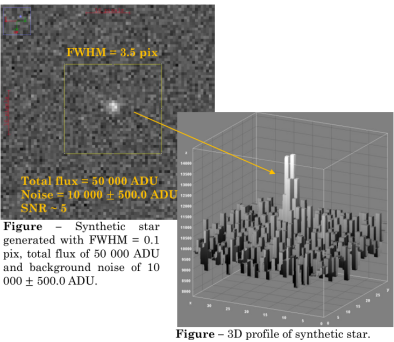
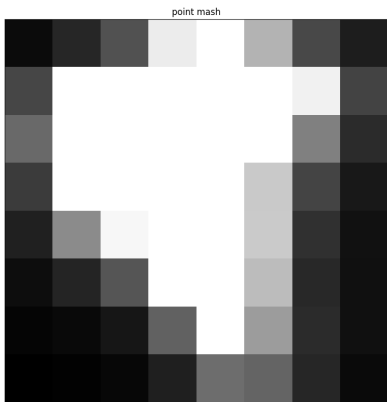
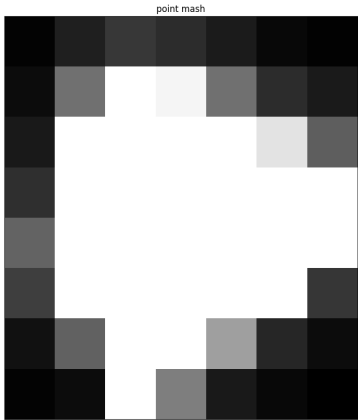


Figure – 3D profile of synthetic star.

Methods

- PSF fitting
- Edge detection
- Barycenter positions

PSF objects detected



PSF fitting - trail

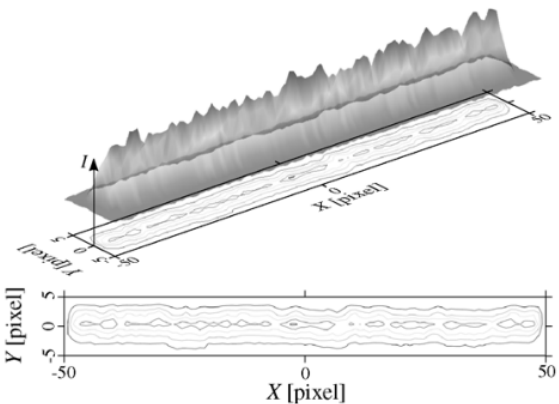


Figure 10: Trail shown from 3d perspective

PSF fitting

$$\begin{aligned} f_T(x, y) = & b(x, y) + \frac{\Phi}{L} \frac{1}{2\sigma\sqrt{2\pi}} \\ & \times \exp \left[-\frac{((x - x_0) \sin \theta + (y - y_0) \cos \theta))^2}{2\sigma^2} \right] \\ & \times \left(\operatorname{erf} \left[\frac{(x - x_0) \cos \theta + (y - y_0) \sin \theta + L/2}{\sigma\sqrt{2}} \right] \right. \\ & \left. - \operatorname{erf} \left[\frac{(x - x_0) \cos \theta + (y - y_0) \sin \theta - L/2}{\sigma\sqrt{2}} \right] \right). \end{aligned}$$

Figure 11: PSF fitting equations

Output

	Type	RA	dRA	Dec.	dDec	R	sR	x	y	Flux	FWHM	Peak	Fit	Designation:-
		h	m	s	.	mag	mag			ADU	*	SNR	RMS	
1	R	28	31	59.109	+0.20	+07 40 13.53	-0.03	12.95	+0.22	1011.38	554.74	15143	6.0	38.7 0.050
2	R	28	31	59.313	(-7.47)	+07 29 29.45	(-1.77)	14.28	-0.71	1605.57	939.81	4790	6.6	12.0 0.126
3	R	28	32	00.108	+0.23	+07 53 07.55	-0.24	13.68	+0.20	1607.48	91.93	8317	6.4	21.1 0.058
4	R	28	32	01.001	-0.16	+07 44 34.44	+0.23	15.97	+0.85	996.24	398.60	939	5.6	7.6 0.134
5	R	28	32	01.718	-0.17	+07 52 09.64	-0.40	14.84	+0.65	992.79	126.41	2662	6.3	11.7 0.087
6	R	28	32	02.164	+0.14	+07 36 42.17	-0.01	14.35	+0.53	982.90	680.85	4159	5.8	14.6 0.073
7	R	28	32	02.328	-0.08	+07 44 33.08	+0.35	15.68	-0.03	984.44	399.30	1232	5.7	8.2 0.128
8	R	28	32	02.408	-0.10	+07 36 04.19	+0.04	14.75	+0.23	980.50	783.54	2879	6.3	12.3 0.085
9	R	28	32	03.314	(-1.20)	+07 37 09.04	(+0.22)	15.93	-0.01	972.80	664.68	977	4.2	7.5 0.137
10	R	28	32	03.317	-0.34	+07 51 09.18	+0.01	15.47	+0.36	978.46	138.50	1493	5.6	8.0 0.129
11	R	28	32	03.883	-0.14	+07 32 28.27	+0.03	15.03	+0.61	966.77	832.51	2236	6.6	9.9 0.118
12	R	28	32	03.817	-0.08	+07 43 38.26	-0.02	14.74	-0.42	978.86	431.98	2926	6.1	13.6 0.072
13	S	28	32	03.817	-0.08	+07 43 38.26	14.75			978.86	431.98	2884	6.1	13.5 0.072
14	R	28	32	03.895	(-1.54)	+07 39 51.87	(+0.66)	16.18	+0.73	968.72	567.29	834	4.6	8.1 0.132
15	R	28	32	04.183	(-1.98)	+07 50 52.14	(-2.24)	14.51	(-3.11)	970.41	172.53	3599	6.0	14.0 0.087
16	R	28	32	04.196	-0.34	+07 45 38.88	+0.03	15.92	-0.69	960.51	375.51	6366	5.9	10.0 0.055
17	R	28	32	04.398	-0.08	+07 45 12.98	+0.03	13.94		966.31	376.33	6073	5.7	19.8 0.053
18	R	28	32	04.566	-0.41	+07 32 05.57	+0.03	14.88	+0.47	959.86	846.01	2557	6.2	18.7 0.112
19	R	28	32	05.083	+0.31	+07 43 44.23	-0.04	12.98	+0.20	959.65	428.27	15820	5.6	32.6 0.046
20	R	28	32	05.384	-0.22	+07 37 19.27	+0.57	14.32	+0.71	955.24	658.48	4296	7.0	13.8 0.097
21	R	28	32	05.370	-0.05	+07 38 13.49	+0.14	15.07	+0.46	954.24	697.72	2143	6.0	9.9 0.122
22	R	28	32	05.461	-0.05	+07 31 16.49	-0.07	13.59	+0.19	951.60	875.33	8421	7.1	28.2 0.067
23	R	28	32	05.478	-0.06	+07 51 17.76	-0.03	14.47	-0.57	959.89	157.18	3737	6.1	14.0 0.070
24	R	28	32	06.189	-0.18	+07 48 23.86	+0.04	9.58	+0.03	951.62	261.98	365175	6.1	156.4 0.032
25	R	28	32	06.310	-0.43	+07 55 17.45	+0.00	8.82	+0.17	953.22	13.75	688917	6.5	194.5 0.046
26	R	28	32	06.569	-0.09	+07 37 56.46	-0.12	13.91	+0.17	944.24	636.06	6237	6.2	19.3 0.068
27	R	28	32	06.698	-0.27	+07 40 47.29	-0.10	12.82	-0.84	945.04	533.93	17021	5.9	34.5 0.048
28	R	28	32	06.621	-0.08	+07 31 46.64	+0.05	13.81	+0.39	941.48	857.16	6873	6.9	17.7 0.068
29	R	28	32	06.685	-0.22	+07 53 08.20	-0.04	15.29	+0.30	949.05	90.98	1762	6.9	7.6 0.147
30	R	28	32	06.892	-0.26	+07 47 09.29	+0.01	14.03	-0.11	944.89	385.52	5587	5.6	18.6 0.055
31	R	28	32	07.033	-0.16	+07 28 46.00	+0.10	13.58	+0.08	936.72	965.12	9091	7.2	19.7 0.076
32	R	28	32	07.092	-0.58	+07 53 37.31	-0.27	15.57	+0.74	945.62	73.54	1354	5.8	8.0 0.128
33	R	28	32	07.655	-0.45	+07 33 29.07	-0.17	14.62	+0.48	932.91	795.82	3258	6.9	12.6 0.083
34	R	28	32	08.213	-0.14	+07 35 24.27	-0.06	13.41	+0.05	928.67	726.91	9937	6.4	23.9 0.053
35	R	28	32	08.461	-0.19	+07 36 48.13	-0.08	14.83	+0.66	926.99	676.75	2679	6.3	12.4 0.096
36	R	28	32	08.815	-0.14	+07 40 08.45	-0.09	13.69	+0.14	925.11	556.95	7633	5.9	21.9 0.052
37	R	28	32	09.927	-0.21	+07 46 14.03	-0.06	13.81	-0.17	917.57	338.30	883	5.7	21.5 0.049
38	R	28	32	18.245	-0.33	+07 45 01.46	-0.00	13.68	-0.35	914.28	381.65	8317	5.7	23.9 0.044
39	R	28	32	18.458	-0.06	+07 38 17.96	-0.10	13.91	-0.25	909.81	623.11	8268	6.1	19.4 0.055

utf-8(dos) 0% 1 / 485 in : 1 [edit] [refresh]

Figure 12: Final result, .cat file

Python

- Numpy
- Astropy (fits files)
- Scipy (convolve, fitting)
- Matplotlib
- OpenCV
- Plotly
- AstroImageJ

Sources

- Heiner Klinkrad - Space Debris, Models and Risk Analysis
- Vladimir Kouprianov et. al. - Distinguishing features of CCD astrometry of faint GEO objects
- J. Šilha et. al. - Slovakian Optical Sensor for HAMR Objects Cataloguing and Research
- Jenni Virtanen et. al. - Streak detection and analysis pipeline for space-debris optical images
- Peter Vereš et. al. - Improved Asteroid Astrometry and Photometry with Trail Fitting
- Oddelenie astronómie a Astrofyziky - Fakulta matematiky fyziky a informatiky, UK
- Edith Stöveken et. al. - Algorithms for the Optical Detection of Space Debris Objects

The End

Thank you for your attention